PNAS RESEARCH ARTICLE | CHEMISTRY

A hybrid meta on-top functional for multiconfiguration pair-density functional theory

Jie J. Bao[a,b], Dayou Zhang[a,b], Shaoting Zhang[a,c], Laura Gagliardi[d,e,1], and Donald G. Truhlar[a,b,1]

Affiliations are included on p. 7.

Contributed by Donald G. Truhlar; received October 3, 2024; accepted November 11, 2024; reviewed by Peter M. Gill and Kirk A. Peterson

Multiconfiguration pair-density functional theory (MC-PDFT) was proposed a decade ago, but it is still in the early stage of density functional development. MC-PDFT uses functionals that are called on-top functionals; they depend on the density and the on-top pair density. Most MC-PDFT calculations to date have been unoptimized translations of generalized gradient approximations (GGAs) of Kohn–Sham density functional theory (KS-DFT). A hybrid MC-PDFT has also been developed, in which one includes a fraction of the complete active space self-consistent-field wave function energy in the total energy. Meta-GGA functionals, which use kinetic-energy densities in addition to GGA ingredients, have shown higher accuracy than GGAs in KS-DFT, yet the translation of meta-GGAs has not been previously proposed for MC-PDFT. In this paper, we propose a way to include kinetic energy density in a hybrid on-top functional for MC-PDFT, and we optimize the parameters of the resulting functional by training with a database developed as part of the present work that contains a wide variety of systems with diverse characters. The resulting hybrid meta functional is called the MC23 functional. We find that MC23 has improved performance as compared to KS-DFT functionals for both strongly and weakly correlated systems. We recommend MC23 for future MC-PDFT calculations.

database | density functional theory | MC-PDFT | meta-GGA | strong correlation

Significance

Multiconfiguration pair-density functional theory (MC-PDFT) is more robust than Kohn–Sham density functional theory (KS-DFT) because it uses a multiconfigurational reference wave function (WF). The independent variables in MC-PDFT density functionals have previously been limited to electron density, on-top pair density, their gradients, and a percentage of complete active space self-consistent field (CASSCF) energy, and the functionals have not been broadly optimized. This paper presents a more accurate functional, called MC23, by introducing kinetic energy density and nonlinearly optimizing a parameterized functional for hybrid MC-PDFT with this additional ingredient. The functional shows systematic improvement compared with currently used MC-PDFT and KS-DFT functionals, as well as with a widely used WF method, namely complete active-space second-order perturbation theory (CASPT2).

The development of well-designed density functional approximations (DFAs) in Kohn–Sham density functional theory (KS-DFT) (1, 2) for electronic structure calculations has revolutionized quantum mechanical simulation because they make it possible to achieve accuracy higher than other comparably expensive methods. The earliest chemically successful DFAs were gradient approximations (GAs), such as PBE (references for all DFAs mentioned in this paper are in *SI Appendix*), BLYP, HCTH, and GAM, which use electron densities and density gradients as their ingredients. These are examples of local functionals in which the energy density at a point in space depends on the ingredients at that point. Hartree–Fock (HF) exchange, which is nonlocal, can be combined with local ingredients to give hybrid DFAs, such as the popular B3LYP. One can also include nonlocal correlation, resulting in doubly hybrid functionals, density-dependent nonlocal correlation, resulting in van der Waals functionals, or correlation terms involving the density coherence, resulting in rung-3.5 functionals.

Among the local ingredients proposed in the context of KS-DFT, arguably the most powerful has been kinetic energy density. Functionals that include kinetic energy densities are called meta functionals. Modern meta functionals originated from attempts to approximate the HF exchange energy in terms of the 1-particle reduced density matrix (1-RDM) (3–6). This led in later work to the use of the kinetic energy density as an ingredient to go along with the density and the density gradient in more general approximations to the exchange–correlation energy (7–11). The kinetic energy density ingredient is closely related to using Laplacians of densities (12–16), and functionals that use Laplacians of the density are also called meta functionals. Examples of meta-DFAs are τ-HCTH, M06-L, MN12-L, MN15-L, and revM06-L. In addition, meta-DFAs can also include a fraction of HF exchange; examples of hybrid meta functionals are TPSSh, M06, MN15, revM06, revM11, and CF22D. The accuracy of many of these functionals is due not only to their broad set of ingredients but also due to broad databases against which parameters are optimized.

A feature that contributes to the widespread use of KS-DFT is that it uses a single Slater determinant as a reference wave function (WF) to compute the total energy, and the simplicity of this approach enables KS-DFT to be used as a black-box method where only the basis set and the DFA need to be chosen. However, a single Slater determinant does not provide a physically correct description of strongly correlated systems, which may be defined as systems for which a single configuration state function (which is a spin-adapted combination of one or more Slater determinants) does not provide a good zero-order

Author contributions: J.J.B., D.Z., L.G., and D.G.T. designed research; S.Z. performed research; J.J.B., D.Z., L.G., and D.G.T. analyzed data; J.J.B. and D.Z. performed the calculations; S.Z. performed some of the calculations; and J.J.B., D.Z., L.G., and D.G.T. wrote the paper.

Reviewers: P.M.G., The University of Sydney; and K.A.P., Washington State University.

Competing interest statement: P.M.G. (reviewer) and L.G. (coauthor) were coauthors of a review article in 2022.

[1]To whom correspondence may be addressed. Email: lgagliardi@uchicago.edu or truhlar@umn.edu.

This article contains supporting information online at https://www.pnas.org/lookup/suppl/doi:10.1073/pnas.2419413121/-/DCSupplemental.

Published December 30, 2024.

description. (Strongly correlated systems are also called multireference systems or inherently multiconfigurational systems, and strong correlation is also called static correlation and near-degeneracy correlation.) As a result of the single-determinant limitation, KS-DFT is expected to have higher accuracy (with presently available DFAs) for weakly correlated systems than for strongly correlated ones (17, 18). With presently available DFAs, KS-DFT can treat some multireference systems well, but often only by breaking spin symmetry, which involves modeling the system with effective spin densities that do not actually represent spin densities but are probably better thought of as unpaired densities. To emphasize this, we sometimes call the effective spin densities ρ_a and ρ_b rather than ρ_α and ρ_β, and in the rest of this article, we use subscripts a and b for all effective quantities (effective spin densities, gradients, and kinetic energy densities).

Multiconfiguration nonclassical-energy functional theory (MC-NEFT) (19–24) is an alternative density functional approach that is designed to treat strongly correlated systems and weakly correlated systems equally well. The original MC-NEFT was multiconfiguration pair-density functional theory (MC-PDFT), and that will be used here. In MC-PDFT calculations, one obtains the classical energy (kinetic energy, nuclear attraction, and classical Coulomb energy of the electrons) from a spin-adapted multiconfigurational WF and then uses an on-top pair-density functional to obtain the nonclassical energy (NE, often called the exchange–correlation energy) as a functional of ingredients evaluated with the reference WF. In work carried out to date, the reference WF is often a complete active space self-consistent-field (CASSCF) WF (25), and the ingredients of the on-top functional are the total density ($\rho \equiv \rho_\alpha + \rho_\beta$), its gradient ($\nabla\rho$), and the on-top pair density (Π). The restricted-active-space, generalized-active-space, and density-matrix renormalization-group WFs have also been used as reference WFs. In order to utilize the physics already built into KS exchange–correlation functionals, the ρ, $\nabla\rho$, and Π ingredients have been translated into effective spin densities ρ_a and ρ_b and effective spin density gradients (which are not necessarily the gradients of the effective spin densities), which are then plugged into a KS functional without reoptimization. For example, our most widely used on-top functional has been translated PBE (tPBE), with effective spin densities and effective gradients obtained by translation and used with the PBE functional form. We have also used a hybrid functional called tPBE0 in which we mix the tPBE energy with a percentage of the CASSCF energy. Although tPBE and tPBE0 are successful, the objective of the present paper is to do better in two ways, namely we add effective spin-resolved kinetic energy densities as new ingredients and we optimize the parameters rather than carrying over a KS functional form with fixed parameters.

The accuracy of tPBE and tPBE0 (when we say tPBE and tPBE0, depending on the context, we are referring to either the translated functional or to an MC-PDFT calculation using it) is similar to second-order complete active space perturbation theory (CASPT2) (26) for bond energies (27, 28), spin splitting (29–32), and excitation energies (33–37). Yet, the cost (as measured by computer time and memory) of running an MC-PDFT calculation is only marginally higher than the cost of CASSCF, whereas the cost of a CASPT2 calculation can be much higher, often unaffordably high when the active space is large, such as 14 electrons in 14 orbitals.

Despite the good accuracy of the tPBE functional, which has been used for the majority of MC-PDFT calculations, it uses the PBE functional form without reoptimization for the present context. Therefore, there is no doubt that it can be improved, and some work has been published that improves or tries to improve the accuracy of MC-PDFT by this route, for example, by mixing the reference WF energy with the MC-PDFT energy to produce hybrid MC-PDFT (38, 39), by introducing the cross-entropy contribution (40), or by introducing a long-range correction for dynamic correlation (41). Here, we examine another direction of improving MC-PDFT's accuracy—namely by including kinetic energy density as well as density, density gradient, on-top pair density, and a percentage of CASSCF energy into the on-top functional. As mentioned above, in KS theory, a functional that includes kinetic energy density is called a meta functional (8), and we will use that notation here as well. Section 1 presents the functional form we use to include kinetic energy density. We optimized parameters in the proposed functional form, and the resulting hybrid meta on-top functional is called MC23.

1. The Functional

In KS-DFT, open-shell and strongly correlated systems are treated with effective spin densities ρ_a and ρ_b, whose sum is the total density ρ. The effective spin densities are obtained from Slater determinants. They should not be interpreted as real spin densities (42, 43), but rather they are unphysical intermediate functions that serve as independent variables upon which the exchange–correlation depends. They are useful for this purpose because their deviation from $\rho/2$ serves as an indication of the open-shell and/or multiconfigurational character of the electronic structure. Using ρ_a^{t} and ρ_b^{t} for effective spin densities obtained by translation (t), g_a^{t} and g_b^{t} for effective spin density gradients obtained by translation, and τ_a^{t}, and τ_b^{t} for effective spin-resolved kinetic energy densities obtained by translation, our goal in the present work is to obtain these intermediate variables from ρ, τ, and Π of a multiconfigurational WF and optimize an NE functional of these nonphysical ingredients for use in hybrid meta MC-PDFT calculations. We need to make two kinds of design choices: i) What form does the on-top energy take as a functional of ρ_a^{t}, ρ_b^{t}, g_a^{t}, g_b^{t}, τ_a^{t}, and τ_b^{t}? ii) How do ρ_a^{t}, ρ_b^{t}, g_a^{t}, g_b^{t}, τ_a^{t}, and τ_b^{t} depend on ρ, τ, and Π? These questions are addressed in Sections 1.1 and 1.2, respectively.

1.1. Form of the Functional. The original approach taken in MC-PDFT was to obtain NE functionals from GA functionals by defining intermediate variables ρ_a^{t}, ρ_b^{t}, g_a^{t}, and g_b^{t} in terms of ρ, $\nabla\rho$, and Π evaluated using the CASSCF reference WF (or more general MCSCF WF) and then making the on-top functional have the same dependence on ρ_a^{t}, ρ_b^{t}, g_a^{t}, and g_b^{t} that the GGA functional has on ρ_a, ρ_b, $|\nabla_{\mathbf{r}}\rho_a|$, and $|\nabla_{\mathbf{r}}\rho_b|$, where $\nabla_{\mathbf{r}}$ is the gradient with respect to the electron coordinate $\mathbf{r}$ (19).

In the present work, we retain these definitions for ρ_a^{t}, ρ_b^{t}, g_a^{t} and g_b^{t}, and we define τ_a^{t} and τ_b^{t} in terms of ρ, Π, and τ, where τ is the kinetic energy density evaluated from the CASSCF reference WF. Meta functionals considered in this article use gradients of orbitals rather than Laplacians of densities, and τ is defined by

$$\tau = \frac{1}{2}\sum_{pq} D_{pq}\nabla_{\mathbf{r}}\phi_p\nabla_{\mathbf{r}}\phi_q. \qquad [1]$$

In KS-DFT, D_{pq} is an element of the 1-RDM computed from the reference Slater determinant, whereas in MC-NEFT, D_{pq} is computed from a multiconfiguration reference WF. In the present work, the multiconfiguration reference WFs are CASSCF functions. Notice that ρ_a^{t}, ρ_b^{t}, g_a^{t}, g_b^{t}, τ_a^{t}, τ_b^{t}, ρ, Π, R, ζ, τ, ϕ_p, and ϕ_q

are all functions of the location **r** where the electron density is evaluated, whereas D_{pq} is independent of **r**.

Then, we make the on-top functional have the same dependence on ρ_a^t, ρ_b^t, g_a^t, g_b^t, τ_a^t, and τ_b^t, that a chosen meta GGA functional form has on ρ_a, ρ_b, $|\nabla_{\mathbf{r}}\rho_a|$, $|\nabla_{\mathbf{r}}\rho_b|$, τ_a, and τ_b. For the present work, for comparison to MC23, we also examine two translated meta on-top functionals in which we do not reoptimize the parameters of the original meta GGA functional, namely tM06-L and tτ-HCTH, which are translations of M06-L and τ-HCTH, respectively.

The optimized hybrid meta on-top functional, called MC23, involves a translation of M06-L, inclusion of a percentage X of CASSCF wave-function energy (hybrid MC-PDFT) (39), and optimization of all 38 linear parameters of tM06-L with simultaneous optimization of X.

1.2. Independent Variables. Recall that the translated spin densities are given by

$$\rho_{a/b}^t = \frac{\rho}{2}(1 \pm \zeta), \quad [2]$$

where

$$\zeta = \begin{cases} \sqrt{1-R}, & R \le 1 \\ 0 & R > 1 \end{cases}, \quad [3]$$

and

$$R = \frac{4\Pi}{\rho^2}, \quad [4]$$

and the translated gradient-like quantities are given by

$$g_{a/b}^t = \frac{|\nabla_{\mathbf{r}}\rho|}{2}(1 \pm \zeta). \quad [5]$$

Notice that g_a^t and g_b^t are treated as independent intermediate quantities; they are not the gradients of ρ_a^t and ρ_b^t.

By analogy to Eqs. **3** and **5**, we define τ_a^t and τ_b^t by

$$\tau_{a/b}^t = \frac{\tau}{2}(1 \pm \zeta). \quad [6]$$

We also justify Eq. **6** from a more theoretical perspective in *SI Appendix*. section S3.

2. Datasets

Because the generation of multiconfigurational WFs requires more work than generating KS reference WFs, we do not include as many systems in each database as are used in our recent optimizations of exchange–correlation functionals for CF22D. We used two collections of databases for optimizing functionals. The first one is dataset 2 (DS2) from our previously published work (24), which is based on the Minnesota Database 2019 (44). The second one is developed for this paper, and we refer to it as Dataset 3 (DS3). Each database consists of several databases having two or more data points. The systems in each database are selected such that they cover as many elements and molecular structures as possible.

Each database has a name of the form *Abbrev-TypeCount* or *TypeCount* where *Count* is the number of systems in the database, *Type* describes the physical or chemical change, and *Abbrev* (which is optional) characterizes the systems in the database For example, AC-DE5 has 5 data, each of which is the dimerization energy ("DE") of an aluminum complex ("AC") [this database is a subset of the Al2X6 database (45) used previously]. An exception is SIE4x4, which contains four data points on each of four potential curves of systems with a delocalized electron and hole, and this database uses the name that was used in previous work (*SI Appendix*, Table S2).

The systems in DS2 are identical to those in ref. 24, except that we removed FeH because the previously used reference value of the FeH bond energy is questionable. Furthermore, we renamed the databases in DS2 according to the consistent naming convention explained above, and the renaming reduced the number of named databases (subdatabases of DS2) from 25 to 24.

In DS3, we include additional systems from Minnesota Database 2019 (44) that are not in DS2, as well as several new databases (created as part of the present work) that were not used previously. (Note that the subdatabases of DS2 and DS3 are also called databases.) For example, the G2-BE5 database, which is the bond energy of five group-2-element dimers, is new.

The number of systems in each subdatabase is shown in panel *A* of Fig. 1, where the databases are grouped by their type. This grouping of databases is also used in Section 4.3. A description of each database is in *SI Appendix*, Table S2. For those databases that represent subsets of databases used in previous work, *SI Appendix*, Table S2 also identifies the parent databases. The systems in each database used here and the reference values of all systems are provided in *SI Appendix*, Tables S3 and S4.

3. Functional Optimization

In optimizing MC23, the first step was calculating the rms error (RMSE) of 18 previously available methods for each of the 28 databases. The methods are CASSCF, CASPT2, tPBE, tPBE0, tτ-HCTH, tM06-L, six KS functional that do not involve kinetic energy density (PBE, PBE0, B1LYP, B3LYP, BLYP, and HCTH) and six that do (τ-HCTH, M06-L, M06, MN15-L, MN15, and CF22D). We then ranked the RMSEs for each database; the lowest RMSE has rank 1, second lowest has rank 2, etc. These ranks were then fit to a piecewise cubic Hermite interpolating polynomial (PCHIP) (46) function, which is monotonic and has smooth first-order derivatives, to connect the ranks of the methods. The PCHIP function for database d as a function of RMSE is called the fractional ranking (R_d) of the RMSE (D_d) for database d; see Fig. 2 as an example. The reason for turning the integer ranks into a continuous function is that we need a continuous function to do optimization.

We note that the PCHIP function does not include the MC23 rank. However, in the analysis of the results presented below, we do include the rank of the final MC23 functional so the number of ranks is increased from 18 to 19, and the ranks of all the methods are reevaluated among 19 methods.

At each stage of the optimization, we computed the RMSE for the new functional on each of these databases, and we call this r_d. The optimization process then seeks the minimum of

$$U = \sum_{d=1}^{28} R_d(r_d) + \lambda \sum_{j=1}^{38} k_j^2 \quad [7]$$

where k_j is one of the optimized parameters of the M06-L functional form (Sections 1.1 and 4.1), and λ is a smoothing parameter to avoid overfitting. By trial and error, we settled on $\lambda = 0.01$ as a good compromise of accuracy and smoothness of the fitted functional. Details of functional optimization are explained in *SI Appendix*, section S5, together with computational details for generating data.

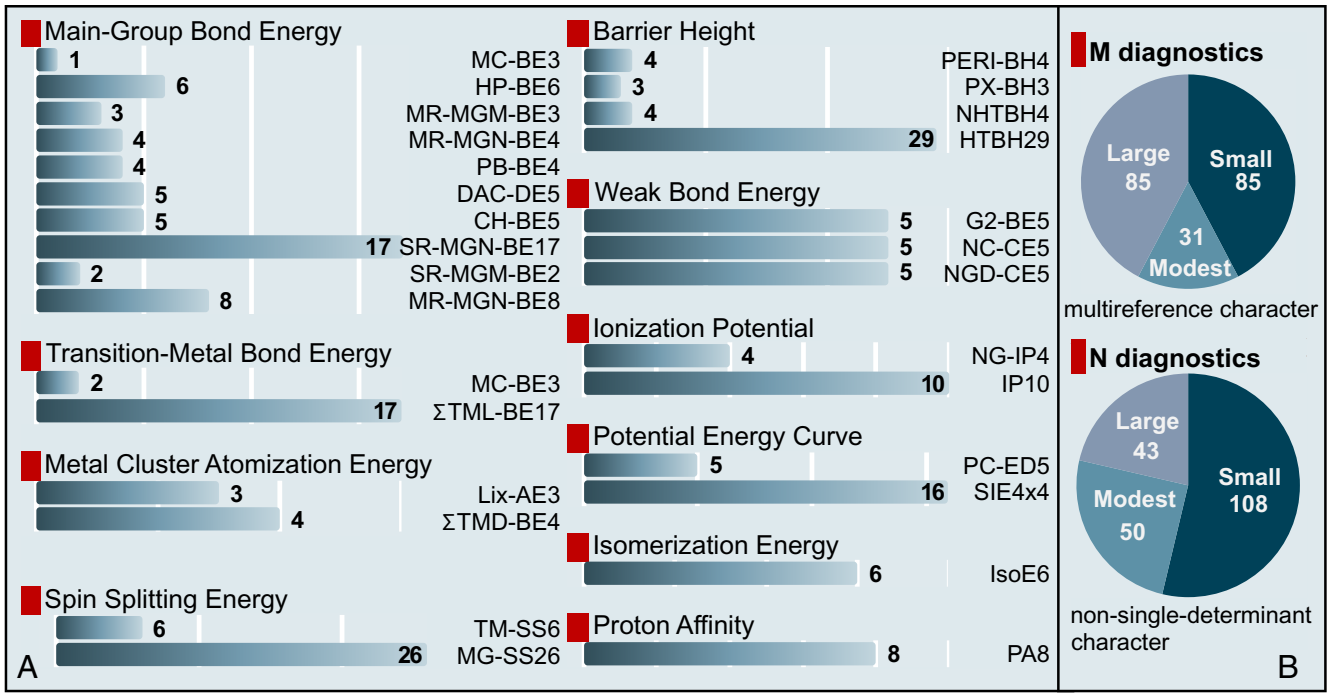

Fig. 1. (*A*) The 28 databases and number of data points in each database grouped according to their type. Note that MC-BE3 occurs twice, as one datum in it is for a main-group bond energy and the other two data are for transition-metal bond energies. (*B*) Data points in 28 databases regrouped according to the multireference diagnostics and non-single-determinant diagnostics. Discussed in Section 4.4.

4. Results and Discussion

4.1. Parameters in MC23. The parameters in the MC23 functional can be found in Table 1. The meaning of each parameter can be found in ref. 47.

4.2. Performance of MC23 and Other Functionals on Each Database. For each of the 19 methods (MC23 and the 18 comparison methods), we averaged over its integer rank on the 28 individual databases. The integer ranks for this purpose are computed using mean unsigned errors (MUEs) with the lower ranks corresponding to smaller MUEs, and the average of these integer ranks are nonintegral average ranks shown in Fig. 3. Although we used RMSEs during optimization because they are smoother functions of the optimized parameters, here we use MUEs because they are more robust for small or nonnormal samples. Fig. 3 shows that MC23 is very successful in ranking highly on each of the databases; this shows that our goal of making a broadly applicable functional was successful.

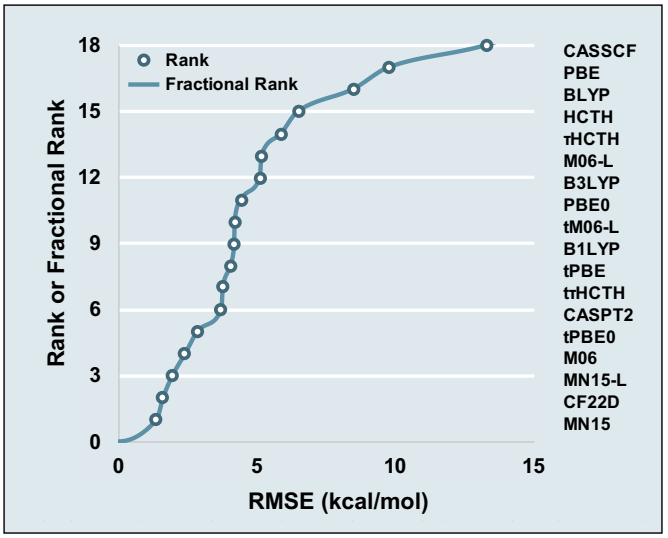

Fig. 2. The PCHIP function of the HTBH29 database.

Fig. 3 shows that MC23 is much more accurate than CASPT2. This is a multireference version of previous experience showing that KS-DFT with modern functionals is much more accurate than MP2 for most properties [see, for example, a previous study (48) of barrier heights where the best KS-DFT functional had an MUE of 0.9 kcal/mol, whereas the various MP2 calculations (which differ in the choice of basis set) had MUEs of 5.0 to 9.3 kcal/mol]. Fig. 3 also shows that the original tPBE functional is comparable to CASPT2 in accuracy, as the MC-PDFT research of the last 10 y has demonstrated.

Table 2 shows that the recent KS CF22D functional does quite well, but not as well as MC23. *SI Appendix*, Tables S8–S10 show that except for MC23, CF22D has the most databases with an MUE below 2 kcal/mol and the least databases with an MUE above 4 kcal/mol. The tPBE method has similar performance to CASPT2, as was stated in our previous work; 20,21 and in particular, if we temporarily exclude SIE4x4, they both have 6 databases with MUEs below 2 kcal/mol, 9 with MUEs in the 2 to 4 range, and 12 with MUEs above 4, in contrast to MC23 with 17, 7, and 3 databases in these respective ranges (full details of MUEs for individual databases are in *SI Appendix*, Tables S8–S10). The very widely used PBE and B3LYP functionals do relatively worse against this difficult set of databases.

A perhaps surprising observation in Table 2 is that CASPT2 has a significantly larger error and worse rank on the large-M and large-N data than on the other data. Even though CASPT2 was originally formulated to improve performance on multireference systems, it does not perform as well for these difficult data as do the KS meta functionals in Table 2 (M06, MN15, and CF22D) or either MC-PDFT functional (tPBE and MC23).

Table 1. Parameters of MC23

	MC23					
	Exchange		Correlation			
i	a_i	d_i	$c_{c\alpha\beta,i}$	$c_{c\sigma\sigma,i}$	$d_{c\alpha\beta,i}$	$d_{c\sigma\sigma,i}$
0	5.908669e+00	−4.962769e+00	1.752729e+00	3.120710e+00	9.700127e−01	−3.362215e+00
1	6.065270e−01	−2.157589e−02	−1.442593e+00	5.394115e+00	−5.922996e−02	7.113888e−02
2	−8.855500e−01	7.272881e−03	−3.099927e+00	−1.219080e+01	4.218804e−02	1.088333e−01
3	4.066804e−01	−3.666348e−05	−4.816831e+00	−1.330073e+00	3.649059e−04	−9.210661e−04
4	1.185208e+00	4.011115e−05	−6.388593e−01	6.366334e+00	1.032979e−03	−3.159415e−03
5	1.040549e+00					
6	7.406380e−01					
7	−2.560799e+00					
8	−9.736623e+00					
9	3.433661e+00					
10	8.193896e+00					
11	−1.261694e+00					
X			28.56			

It is shown in Fig. 3 and *SI Appendix*, Tables S11 and S13 that tM06-L is less broadly accurate than M06-L, and tτ-HCTH is less broadly accurate than τ-HCTH, although tPBE is more broadly accurate than PBE. This shows the necessity of reoptimizing a functional in the MC-PDFT framework if one pursues high accuracy with modern functionals.

We notice in *SI Appendix*, Tables S8–S10 that 16 of the 19 considered methods have large errors of 10.2 to 24.5 kal/mol on the SIE4x4 database, which consists of systems like He_2^+ and H_2^+ that are notoriously difficult for density functional theories. CASPT2, CASSCF, and MC23 have respective errors of 3.3, 7.2, and 9.4 kcal/mol for SIE4x4.

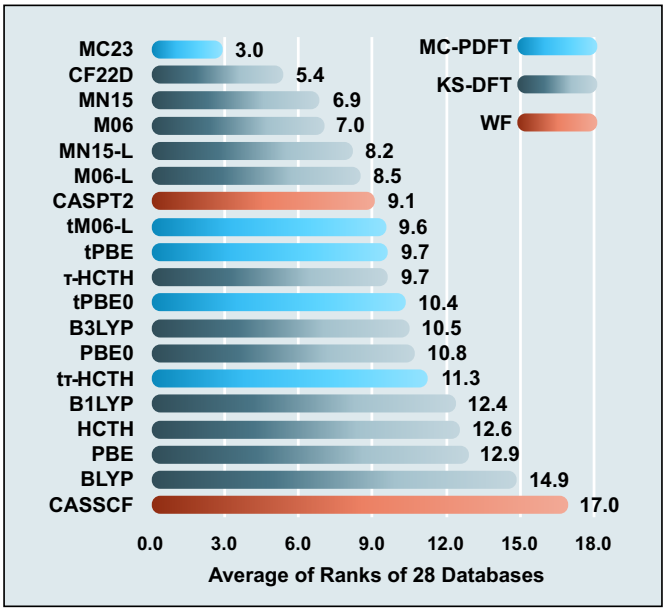

Fig. 3. Ranks for each MC-PDFT functional, KS-DFT functional, and WF method averaged over 28 databases (from the last rows of *SI Appendix*, Tables S11–S13).

4.3. Performance of MC23 and Other Functionals on Regrouped Databases. To gain a more coarse-grained perspective, especially in light of the small number of systems in some of the databases, we recombined the data in all databases into the following seven larger databases:

1. MG-BE55 database: main-group bond energies, including data points in MR-MGN-BE8, SR-MGM-BE2, and SR-MGN-BE17 from DS2, as well as DAC-DE5, CH-BE5, HP-BE6, MR-MGM-BE3, MR-MGN-BE4, and PB-BE4 from DS3, plus LiO^- from MC-BE3 in DS2.
2. TM-BE19 database: transition-metal bond energies, including FeCl and CuCl in MC-BE3 from DS2, as well as all data points in ΣTML-BE17 from DS3.
3. MC-AE7 database: metal-cluster atomization energies per atom, including all data points in ΣTMD-BE4 and Lix-AE3 from DS3.
4. BH40 database: barrier heights, including all data points in HTBH29 and NHTBH4 from DS2, as well as PX-BH3 and PERI-BH4 from DS3.
5. WB15 database: weakly bonded and noncovalent complexes, including all data points in NGD-CE5, NC-CE5, and G2-BE5 from DS3.
6. SS32 database: spin-splitting energies, including all data points in MG-SS26 and TM-SS6 from DS3.
7. The "other" database: including 49 data points from IP10, NG-IP4, IsoE6, PA8, SIE4x4, and PC-ED5 from DS3.

For eight methods selected for illustration, Table 3 presents the MUE averaged over data points in each regrouped database, and it also shows the ranks of these MUEs, where the ranks are based on the full set of 19 methods (MUEs and ranks of all methods can be found in *SI Appendix*, Tables S14 and S15).

Table 2 shows that MC23 is the most accurate or second-most accurate method for all regrouped databases except BH40 and the "other" database. For barrier heights, the MUE for MC23 is 0.9 kcal/mol

Table 2. MUE (kcal/mol) over data categorized by multireference character for 10 methods and their ranks[*,†]

	MC-PDFT			KS-DFT				
	MC23	tPBE	CASPT2	PBE	B3LYP	M06	MN15	CF22D
MUE								
SmallM85	2.2	4.1	3.2	6.2	4.5	2.5	2.5	2.0
ModerateM31	3.3	3.4	3.1	7.5	5.0	3.5	3.5	2.4
LargeM85	2.6	4.4	5.1	6.9	5.7	4.1	4.3	4.3
SmallN108	2.2	4.3	3.5	6.5	5.5	2.8	3.1	2.6
ModerateN50	3.1	3.7	4.4	7.3	4.5	3.6	3.6	2.8
LargeN43	2.7	4.1	4.7	6.4	4.7	4.4	4.1	4.7
Rank								
SmallM85	2	12	6	17	15	3	4	1
ModerateM31	3	5	2	18	13	7	6	1
LargeM85	1	8	12	17	14	2	7	6
SmallN108	1	10	5	17	15	3	4	2
ModerateN50	2	6	7	18	9	5	4	1
LargeN43	1	6	13	18	12	9	7	11

[*]SmallM85 is the collection of the 85 data that have small *M* (<0.05); ModerateM31 is the collection of the 31 data that have moderate *M* (0.05 to 01); LargeM85 is the collection of 85 data that have large *M* (>0.1); SmallN108 is the collection of the 108 data that have small *N* (<0.05); etc.
[†]Rank is over the same 19 methods as considered elsewhere in the article.

higher than the best methods, namely CF22D and MN15, and we think this is a reasonable tradeoff against the higher other accuracies for MC23. We note that a third of the "other" database (16 points out of 49) is from SIE4x4, and we have already discussed the difficulty of SIE4x4 for density functional theory.

4.4. Performance of MC23 and Other Functionals According to Multireference Characters. To examine the accuracy of density functionals for strongly correlated systems, we classify the systems with the M diagnostic (49) and a diagnostic called the N diagnostic that is introduced in this paper. To understand the reason for having two diagnostics, we recall that correlation energy may be measured as exact electronic energy minus either the spin-restricted HF value or the spin-unrestricted HF (UHF) value (50). The difference between these two values (the restricted correlation energy, RCE, and unrestricted correlation energy, UCE) is called type A static correlation energy (51). It represents the portion of the correlation energy that can be recovered by breaking spin symmetry in a UHF calculation.

The M diagnostic is defined as

$$M = \frac{1}{2}\left[2 - N_{\mathrm{MCDOMO}} + N_{\mathrm{MCUMO}} + \sum_{i}^{n_{\mathrm{SOMO}}} \left|N_{\mathrm{SOMO},i} - 1\right|\right], \quad [8]$$

where N_{MCDOMO} is the natural orbital occupation number (NOON) of the most correlated nominally doubly occupied molecular orbital, N_{MCUMO} is the NOON of the most correlated nominally unoccupied molecular orbital, $N_{\mathrm{SOMO},i}$ is the NOON of a nominally singly occupied molecular orbital with an index i, and n_{SOMO} is the total number of singly occupied molecular orbitals. In this formula, the classification of an orbital as doubly occupied, singly occupied, or empty is defined as follows:

Define the number of doubly occupied orbitals in a single-determinantal configuration as $n_{\mathrm{D}} = (n - 2S)/2$, where n is the total number of electrons in the system (molecule or supermolecule) and S is the total electron spin (e.g., S = 1/2 for a doublet), and define the number of singly occupied orbitals as $n_{\mathrm{S}} = 2S$. Then, define nominally doubly-occupied natural orbitals as the n_{D} natural orbitals with the largest NOON, nominally singly occupied natural orbitals as the n_{S} natural orbitals with the next largest NOON, and nominally unoccupied orbitals as all the rest. Finally, N_{MCDOMO} is the NOON of the doubly occupied orbitals that deviates the most from 2, N_{MCUMO} is the NOON of the unoccupied orbital whose NOON deviates the most from 0, and $N_{\mathrm{SOMO},i}$ is the NOON of the i-th SOMO.

This definition is slightly modified from the previous definition (49) in order to handle supermolecules. The modified definition yields the same M as the previous one when there is no supermolecule involved.

The M diagnostic correctly describes the deviation of an MCSCF WF from the best spin-restricted single determinant, and we previously (49) established the convention that $M \le 0.05$ is classified as small multireference character, $0.05 < M < 0.10$ is classified as moderate multireference character, and $M \ge 0.10$ is classified as large multireference character.

Next consider the dissociation of H_2, which can be well described by a CASSCF calculation with two active electrons in two active orbitals. As worked out in detail in *SI Appendix*, this yields $M = 1$, correctly indicating that the multireference character is large when measured by the inability of the state to be well represented by a single spin-restricted Slater determinant. However, a UHF calculation (or an unrestricted KS calculation, even with popular currently available functionals) is qualitatively correct for the breaking of a single bond; therefore, this is type-A correlation. In order to have a measure of multireference character that accounts for the inability of a state to be represented by even a spin-unrestricted single configuration, we define the N diagnostic.

The N diagnostic uses the same formula as the M diagnostic (simply change M to N in Eq. **8**), but with a different categorization

Table 3. MUE (kcal/mol) over seven regrouped databases for eight representative methods and their ranks

	MC-PDFT			KS-DFT				
	MC23	tPBE	CASPT2	PBE	B3LYP	M06	MN15	CF22D
MUE								
MG-BE55	2.1	4.0	5.0	6.3	4.9	2.9	2.6	2.2
TM-BE19	4.4	7.7	4.8	7.1	5.4	7.2	5.3	5.6
MC-AE7	0.9	4.4	4.3	1.6	5.1	3.0	3.5	4.6
BH40	2.3	3.8	2.9	9.3	4.5	1.9	1.4	1.4
WB15	0.3	0.8	0.9	1.6	1.3	0.6	0.4	0.5
SS32	4.7	5.2	5.0	10.2	9.4	5.9	8.8	7.3
other (49)	4.3	7.0	3.5	10.2	8.0	6.2	5.3	4.8
Rank								
MG-BE55	1	9	13	16	12	4	3	2
TM-BE19	1	16	2	14	6	15	4	7
MC-AE7	1	11	10	3	14	7	9	12
BH40	6	12	7	18	14	3	1	2
WB15	2	8	9	17	15	5	3	4
SS32	2	5	3	18	16	6	13	8
other (49)	2	11	1	16	14	7	4	3

of the orbitals to obtain the quantities on the right-hand side. For the N diagnostic, we categorize the doubly occupied orbitals as those whose NOON is greater than or equal to 1.5, the empty orbitals as those whose NOON is less than or equal to 0.5, and the singly occupied orbitals as those whose NOON is between 0.5 and 1.5. Using these categorizations, the N diagnostic of H_2 at dissociation is 0. This shows how the N diagnostic measures whether a system can be well described by the UHF method or by most currently available unrestricted KS functionals, and this is very relevant to developing methods that improve on KS theory for energetic predictions. More details of the two diagnostics are given in *SI Appendix*.

We classified the initial and final states of all data except SIE4x4 in terms of M and N, and the classifications are given in *SI Appendix*, Table S7. Since each datum has an initial and a final state, the diagnostic was assigned as whichever of these is higher. Then, we computed MUEs and ranks (based on MUE) for each category of data. The results for selected methods are in Table 2; MUEs and rankings for all methods are in *SI Appendix*, Tables S16 and S17.

Table 2 shows that MC23 ranks in the top three in all six categories, and MC23 has a lower MUE than CASPT2 for all six categories, including 2.0 kcal/mol lower for large N. We conclude the MC23 is accurate for both weakly correlated and strongly correlated systems with either the M or N diagnostic used to measure multireference character. This is in contrast to hybrid meta KS functionals in the final three columns, which all show decreasing accuracy for both large M and large N. MC23 is the only method in the table that has a smaller MUE for large N than for modest N.

The N diagnostic also allows us to better understand Table 3. Among the databases in Table 3, we see that all three MR methods, namely MC23, tPBE, and CASPT2 have smaller MUEs in the spin-splitting database (SS32) than do the KS-DFT functionals. We propose two reasons for this finding. The first reason is that KS functionals use broken-symmetry Slater-determinants, yielding a spin-contaminated state as a linear combination of spin eigenstates. The second reason is that in some systems, at least one of the two spin states is strongly multiconfigurational and cannot be described by a single determinant. For example, singlet O_2 has an N diagnostic of 0.11, indicating that a single Slater determinant is not a qualitatively good reference WF for this system. A recent work reduced the errors in singlet-triplet gaps by introducing complex translated spin densities (52), so it might be advantageous in future work to employ a complex translation scheme in meta-MC-PDFT or hybrid meta-MC-PDFT functionals.

5. Concluding Remarks

In this paper, we proposed a way to introduce kinetic energy densities into MC-PDFT such that MC-PDFT can use meta functionals. We increased the diversity of our previously published database with automatically selected active spaces by adding additional kinds of data with manually selected active spaces. Based on the expanded set of databases, we optimized a hybrid translated meta functional named MC23. We find that MC23 is accurate for both single-reference and multireference systems, according to both our previously published multireference diagnostic and a diagnostic that measures the inability of a state to be represented by a single determinant, whereas the previously trained state-of-the-art KS functionals do not possess such broad accuracy. We also see improved performance of MC23 compared with KS functionals on spin splitting energies, which is attributed to MC23 using densities from spin-adapted multiconfigurational WFs. We consider a variety of ways of partitioning the data that show that MC23 has broad accuracy across a range of different kinds of systems.

Data, Materials, and Software Availability. The developer's branch of *OpenMolcas* for calculations with MC23 is available open source on GitLab at https://gitlab.com/qq270814845/OpenMolcas (53) commit dbe66bdde53f6d0bc4e9e5bcc0243922b3559a66. Cartesian coordinates, WF files, absolute energies, and the mapping of system names to energy differences for *OpenMolcas* and *Gaussian 16* calculations are available at https://doi.org/10.5281/zenodo.10724676 (54).

ACKNOWLEDGMENTS. We thank Pragya Verma for helpful assistance with the database creation. We thank Matthew Hermes, Daniel King, and Matthew Hennefarth for helpful discussion. This work was supported in part by the Air Force Office of Scientific Research by grant FA9550-20-1-0360.

Author affiliations: [a]Department of Chemistry, Chemical Theory Center, University of Minnesota, Minneapolis, MN 55455-0431; [b]Minnesota Supercomputing Institute, University of Minnesota, Minneapolis, MN 55455-0431; [c]College of Chemistry, Nankai University, Tianjin 300071, China; [d]Department of Chemistry, Pritzker School of Molecular Engineering, James Franck Institute, The University of Chicago, Chicago, IL 60637; and [e]Chicago Center for Theoretical Chemistry, The University of Chicago, Chicago, IL 60637

1. W. Kohn, L. J. Sham, Self-consistent equations including exchange and correlation effects. *Phys. Rev.* **140**, A1133–A1138 (1965).
2. P. Hohenberg, W. Kohn, Inhomogeneous electron gas. *Phys. Rev.* **136**, B864–B871 (1964).
3. A. D. Becke, M. R. Roussel, Exchange holes in inhomogeneous systems: A coordinate-space model. *Phys. Rev. A* **39**, 3761–3767 (1989).
4. R. M. Koehl, G. K. Odom, G. E. Scuseria, The use of density matrix expansions for calculating molecular exchange energies. *Mol. Phys.* **87**, 835–843 (1996).
5. T. Van Voorhis, G. E. Scuseria, Exchange energy functionals based on the density matrix expansion of the Hartree-Fock exchange term. *Mol. Phys.* **92**, 601–608 (1997).
6. T. Van Voorhis, G. E. Scuseria, A novel form for the exchange-correlation energy functional. *J. Chem. Phys.* **109**, 400–410 (1998).
7. A. D. Becke, A new inhomogeneity parameter in density-functional theory. *J. Chem. Phys.* **109**, 2092–2098 (1998).
8. J. P. Perdew *et al.*, Accurate density functional with correct formal properties: A step beyond the generalized gradient approximation. *Phys. Rev. Lett.* **82**, 2544–2547 (1999).
9. M. Ernzerhof, G. E. Scuseria, Kinetic energy density dependent approximations to the exchange energy. *J. Chem. Phys.* **111**, 911–915 (1999).
10. A. D. Boese, N. C. Handy, New exchange-correlation density functionals: The role of the kinetic-energy density. *J. Chem. Phys.* **116**, 9559–9569 (2002).
11. Y. Zhao, D. G. Truhlar, Design of density functionals that are broadly accurate for thermochemistry, thermochemical kinetics, and nonbonded interactions. *J. Phys. Chem. A* **109**, 5656–5667 (2005).
12. E. Proynov, A. Vela, D. Salahub, Nonlocal correlation functional involving the Laplacian of the density. *Chem. Phys. Lett.* **230**, 419–428 (1994).
13. A. C. Cancio, M. Y. Chou, Beyond the local approximation to exchange and correlation: The role of the Laplacian of the density in the energy density of Si. *Phys. Rev. B* **74**, 081202 (2006).
14. J. P. Perdew, L. A. Constantin, Laplacian-level density functionals for the kinetic energy density and exchange-correlation energy. *Phys. Rev. B* **75**, 155109 (2007).
15. S. Laricchia *et al.*, Laplacian-level kinetic energy approximations based on the fourth-order gradient expansion: Global assessment and application to the subsystem formulation of density functional theory. *J. Chem. Theory Comput.* **10**, 164–179 (2014).
16. S. Śmiga *et al.*, Laplacian-dependent models of the kinetic energy density: Applications in subsystem density functional theory with meta-generalized gradient approximation functionals. *J. Chem. Phys.* **146**, 064105 (2017).
17. P. Verma, D. G. Truhlar, Status and challenges of density functional theory. *Trends Chem.* **2**, 302–318 (2020).
18. Y. Zhao, D. G. Truhlar, Density functionals with broad applicability in chemistry. *Acc. Chem. Res.* **41**, 157–167 (2008).
19. G. Li Manni *et al.*, Multiconfiguration pair-density functional theory. *J. Chem. Theory Comput.* **10**, 3669–3680 (2014).
20. L. Gagliardi *et al.*, Multiconfiguration pair-density functional theory: A new way to treat strongly correlated systems. *Acc. Chem. Res.* **50**, 66–73 (2017).
21. P. Sharma *et al.*, Multiconfiguration pair-density functional theory. *Annu. Rev. Phys. Chem.* **72**, 541–564 (2021).
22. D. S. King, D. G. Truhlar, L. Gagliardi, Machine-learned energy functionals for multiconfigurational wave functions. *J. Phys. Chem. Lett.* **12**, 7761–7767 (2021).
23. C. Zhou *et al.*, Electronic structure of strongly correlated systems: Recent developments in multiconfiguration pair-density functional theory and multiconfiguration nonclassical-energy functional theory. *Chem. Sci.* **13**, 7685–7706 (2022).
24. D. Zhang, D. G. Truhlar, An accurate density coherence functional for hybrid multiconfiguration density coherence functional theory. *J. Chem. Theory Comput.* **19**, 6551–6556 (2023).
25. B. O. Roos, The complete active space self-consistent field method and its applications in electronic structure calculations. *Adv. Chem. Phys.* **69**, 399–445 (1987).
26. K. Andersson *et al.*, Second-order perturbation theory with a CASSCF reference function. *J. Phys. Chem.* **94**, 5483–5488 (1990).
27. S. O. Odoh *et al.*, Separated-pair approximation and separated-pair pair-density functional theory. *Chem. Sci.* **7**, 2399–2413 (2016).
28. J. L. Bao *et al.*, Predicting bond dissociation energies of transition-metal compounds by multiconfiguration pair-density functional theory and second-order perturbation theory based on correlated participating orbitals and separated pairs. *J. Chem. Theory Comput.* **13**, 616–626 (2017).
29. J. L. Bao *et al.*, Correlated-participating-orbitals pair-density functional method and application to multiplet energy splittings of main-group divalent radicals. *J. Chem. Theory Comput.* **12**, 4274–4283 (2016).
30. S. J. Stoneburner, D. G. Truhlar, L. Gagliardi, MC-PDFT can calculate singlet–triplet splittings of organic diradicals. *J. Chem. Phys.* **148**, 064108 (2018).
31. S. Ghosh *et al.*, Generalized-active-space pair-density functional theory: An efficient method to study large, strongly correlated, conjugated systems. *Chem. Sci.* **8**, 2741–2750 (2017).
32. L. Wilbraham *et al.*, Multiconfiguration pair-density functional theory predicts spin-state ordering in iron complexes with the same accuracy as complete active space second-order perturbation theory at a significantly reduced computational cost. *J. Phys. Chem. Lett.* **8**, 2026–2030 (2017).
33. S. Ghosh *et al.*, Multiconfiguration pair-density functional theory outperforms Kohn–Sham density functional theory and multireference perturbation theory for ground-state and excited-state charge transfer. *J. Chem. Theory Comput.* **11**, 3643–3649 (2015).
34. C. E. Hoyer *et al.*, Multiconfiguration pair-density functional theory is as accurate as CASPT2 for electronic excitation. *J. Phys. Chem. Lett.* **7**, 586–591 (2016).
35. C. E. Hoyer, L. Gagliardi, D. G. Truhlar, Multiconfiguration pair-density functional theory spectral calculations are stable to adding diffuse basis functions. *J. Phys. Chem. Lett.* **6**, 4184–4188 (2015).
36. S. S. Dong, L. Gagliardi, D. G. Truhlar, Excitation spectra of retinal by multiconfiguration pair-density functional theory. *Phys. Chem. Chem. Phys.* **20**, 7265–7276 (2018).
37. J. J. Bao *et al.*, Automatic selection of an active space for calculating electronic excitation spectra by MS-CASPT2 or MC-PDFT. *J. Chem. Theory Comput.* **14**, 2017–2025 (2018).
38. M. Mostafanejad, M. D. Liebenthal, A. E. DePrince, Global Hybrid multiconfiguration pair-density functional theory. *J. Chem. Theory Comput.* **16**, 2274–2283 (2020).
39. R. Pandharkar *et al.*, A new mixing of nonlocal exchange and nonlocal correlation with multiconfiguration pair-density functional theory. *J. Phys. Chem. Lett.* **11**, 10158–10163 (2020).
40. R. Feng, I. Y. Zhang, X. Xu, Consistent improvement on both exchange and correlation within hybrid multiconfiguration pair-density functional theory: TB4LYP. ChemRxiv [Preprint] (2023). 10.26434/chemrxiv-2023-fgr88. Accessed 27 July 2024.
41. M. Hapka, E. Pastorczak, A. Krzemińska, K. Pernal, Long-range-corrected multiconfiguration density functional with the on-top pair density. *J. Chem. Phys.* **152**, 094102 (2020).
42. M. Reiher, On the definition of local spin in relativistic and nonrelativistic quantum chemistry. *Faraday Discuss.* **135**, 97–124 (2007).
43. D. Zhang, D. G. Truhlar, Multiconfigurational effects on the density coherence. *J. Chem. Theory Comput.* **16**, 6915–6925 (2020).
44. P. Verma, D. G. Truhlar, Geometries for Minnesota database 2019. Data Repository for the University of Minnesota. https://doi.org/10.13020/217y-8g32. Deposited 20 November 2019.
45. L. Goerigk *et al.*, A look at the density functional theory zoo with the advanced GMTKN55 database for general main group thermochemistry, kinetics and noncovalent interactions. *Phys. Chem. Chem. Phys.* **19**, 32184–32215 (2017).
46. F. N. Fritsch, J. Butland, A method for constructing local monotone piecewise cubic interpolants. *SIAM J. Sci. Stat. Comput.* **5**, 300–304 (1984).
47. Y. Zhao, D. G. Truhlar, A new local density functional for main-group thermochemistry, transition metal bonding, thermochemical kinetics, and noncovalent interactions. *J. Chem. Phys.* **125**, 194101 (2006).
48. J. Zheng, Y. Zhao, D. G. Truhlar, The DBH24/08 database and its use to assess electronic structure model chemistries for chemical reaction barrier heights. *J. Chem. Theory Comput.* **5**, 808–821 (2009).
49. O. Tishchenko, J. Zheng, D. G. Truhlar, Multireference model chemistries for thermochemical kinetics. *J. Chem. Theory Comput.* **4**, 1208–1219 (2008).
50. J. Pople, J. Binkley, Correlation energies for AH_n molecules and cations. *Mol. Phys.* **29**, 599–611 (1975).
51. J. W. Hollett, P. M. W. Gill, The two faces of static correlation. *J. Chem. Phys.* **134**, 114111 (2011).
52. G. L. S. Rodrigues, M. Scott, M. G. Delcey, Multiconfigurational pair-density functional theory is more complex than you may think. *J. Phys. Chem. A* **127**, 9381–9388 (2023).
53. J. J. Bao *et al.*, A developer's branch of OpenMolcas. GitLab. https://gitlab.com/qq270814845/OpenMolcas. Accessed 8 January 2024.
54. J. J. Bao, D. Zhang, S. Zhang, L. Gagliardi, D. G. Truhlar, Data set for the development and testing of the MC23 nonclassical-energy functional. Zenodo. https://doi.org/10.5281/ZENODO.10724676. Deposited 20 September 2024.